

Heavy quarkonia in a baryon asymmetric strongly magnetized hot quark matter

Salman Ahamad Khan^{†1}, Mujeeb Hasan^{†2} and Binoy Krishna Patra^{†3}

[†] *Department of Physics, Indian Institute of Technology Roorkee, Roorkee 247 667, India*

Abstract

Recently there is a resurrection in the study of heavy quark bound states in a hot and baryonless matter with an ambient magnetic field but the matter produced at heavy-ion collider experiments is not perfectly baryonless, so we wish to explore the effect of small baryon asymmetry on the in-medium properties of the heavy quark bound states submerged in a strongly magnetized hot quark matter. Therefore, we have first given a revisit to the general covariant tensor structure of gluon self-energy in the above environment to compute the resummed propagator for gluons. This resummed propagator embodies the properties of medium, which gets translated into the (complex) potential between Q and \bar{Q} placed in the medium. We observe that the baryon asymmetry makes the real-part of potential slightly more attractive and weakens the imaginary-part. This opposing effects thus lead to the enhancement of binding energies and the reduction of thermal widths of $Q\bar{Q}$ ground states, respectively. Finally, the properties of quarkonia thus deciphered facilitate to compute the dissociation points of J/ψ and Υ , which are found to have slightly larger values in the presence of baryon asymmetry. For example, J/ψ gets dissociated at $1.64 T_c$, $1.69 T_c$, and $1.75 T_c$, whereas Υ is dissociated at $1.95 T_c$, $1.97 T_c$ and $2.00 T_c$, for $\mu = 0, 60$ and 100 MeV, respectively. This observation prevents early dissociation of quarkonia in the matter produced at ultrarelativistic heavy ion collisions with a small net baryon number, compared to the ideal baryonless matter.

Keywords: Strong magnetic field; Perturbative QCD; Quark chemical potential; Resummed propagator; Heavy quark potential;

¹skhan@ph.iitr.ac.in

²mhasan@ph.iitr.ac.in

³binoy@ph.iitr.ac.in

1 Introduction

In the presence of high temperatures and/or densities, colourless hadrons get melted into a plasma of asymptotically free quarks and gluons known as Quark-Gluon Plasma (QGP). This type of extreme environment is created in the ultrarelativistic heavy-ion collisions (URHICs) experiments at RHIC [1, 2] and LHC [3, 4] and is planned to be created in the Compressed Baryonic Matter (CBM) experiment at Facility for Antiproton and Ion Research (FAIR) [5]. In noncentral events in URHICs, the relative motion of the spectator quarks generates a strong magnetic field (SMF) at initial phases of the collisions. The magnitude of the produced magnetic field (B) is around m_π^2 ($\sim 10^{18}$ Gauss) at RHIC to $10\ m_\pi^2$ at LHC [6, 7]. This strong magnetic field is a short pulse. Earlier, people did not pay much attention to the effects of magnetic field on thermal QCD medium because they thought that the life-span of the strong magnetic field was too short to have any observable effects in the phenomenology of the heavy-ion collisions. They observed that the produced strong magnetic field decays very fast in vacuum. But some recent theoretical calculations predict that a thermal medium could have produced as early as the production of magnetic field. As a consequence, the life span of the magnetic field is elongated due to the finite electrical conductivity of the medium [8–10]. The decay of the magnetic field in medium becomes slower and it remains strong for much larger time. However, its magnitude becomes weaker as the time is elapsed. Many theoretical studies have been conducted in recent years to decode the effects of this intense B on thermal and magnetic properties of QGP [11–14] and chiral and axial magnetic effects [15–18].

The timescale for the generation of the SMF and the heavy quark pairs in URHICs is almost similar. Apart from this, it was found in few studies that a large quark chemical potential (μ) (upto 100 MeV) is also produced near the deconfining temperature [19–21] and in the SMF its strength reaches upto 200 MeV [22]. The experimental set up at FAIR will provide facilities to investigate the rich physics of the deconfined phase of matter at high baryon densities. The study of the effect of baryon asymmetry on the properties of the QCD medium is very interesting and have applications to few branches of cosmology,

the physics of the core of neutron stars, and URHICs. The $Q\bar{Q}$ bound state of the heavy quarks is one of the very promising signatures to visualize the properties of QGP, therefore the study of the effects of baryon asymmetry on $Q\bar{Q}$ potential becomes a necessary task. Two of us recently investigated the $Q\bar{Q}$ potential and dissociation temperatures for the bound states in magnetized QCD medium at zero chemical potential [23]. In present work, we will examine the effects of the finite quark chemical potential on the various properties (binding energy, decay width and dissociation temperature) of $Q\bar{Q}$ bound states.

In past few years, heavy quarkonium physics has seen many developments. To describe the heavy quark bound system, many effective field theories (EFTs) have been derived using the hierarchy of the various scales of $Q\bar{Q}$ system. One of such theory is non-relativistic QCD (NRQCD) [24] which has been formulated by integrating out the mass (m_Q). Similarly, potential NRQCD [25], is derived by integrating out the momentum exchange ($m_Q v$). Since the hierarchy of scales in these effective theories is not very noticeable, lattice QCD approach [26] is formulated to overcome the difficulties in EFTs. In parallel, phenomenological potential models have been also derived which provide an substitute to probe the various properties of the quarkonia. It has been observed in [27] that the $Q\bar{Q}$ potential possess both real as well as imaginary part. The real part gets screened because of the color charges [28] whereas the resonance acquires a thermal width as a result of the imaginary part [29]. Earlier, it was believed that the dissociation of the quarkonia was because of the color screening phenomena but now a days it is well understood that the $Q\bar{Q}$ bound states are dissolved mainly because of the widening of the thermal width either due to Landau damping [27] or color singlet-octet transition [30]. The bound state gets dissociated at lower temperatures (in comparison to the binding energy) even if there is very weak screening present in the medium as a consequence of the imaginary part. One of us has studied the medium modification to imaginary-part by taking both the perturbative and non-perturbative components and has observed that the imaginary part becomes smaller [31,32], compared to the perturbative term alone [33]. The imaginary part has been also calculated in the framework of Gauge-gravity duality in [34,35] and in lattice stud-

ies [36]. The (complex) $Q\bar{Q}$ potential has been explored using the generalized Gauss law in [37] and the divergence in the imaginary-part was tamed by choosing the Debye mass as the regulation scale. In a recent work, the string part of the potential has been calculated through a phenomenological term which includes the effects due to the low frequency modes subsumed in the dimension two gluon condensates [38]. The above mentioned works have been carried out in the absence of the B . The effect of the SMF on the heavy quarkonia has been investigated recently in many groups. The influence of constant external magnetic field on the QCD bound states have been studied for the case of a harmonic interaction and for Cornell potential plus a spin spin interaction term in [39, 40]. The $Q\bar{Q}$ bound states have been extensively investigated in SMF in [41, 42]. Two of us have explored the effects of SMF on the in-medium properties of the $Q\bar{Q}$ bound states in hot medium and studied the dissociation through both color screening and Landau damping phenomenon [23, 43]. Authors in [44] have also investigated the complex $Q\bar{Q}$ potential using the generalized Gauss law. An attempt has been made to study the anisotropic nature of the inter-quark potential in [45] and the dissociation of the heavy quark bound states in the weak magnetic field in [46]. Apart from these works on the $Q\bar{Q}$ bound states, the effects of B on the propagation of the heavy quarks in the thermal QCD medium have been investigated in some other works *like* wakes in [47]. The collisional energy loss in [48] and the anisotropic nature of the diffusion and the drag coefficients using the Langevindynamics in [49]. In addition to this the general structure of the gauge boson two point functions have been investigated in the magnetized hot material medium in [50].

In this article, we will study the implications of the baryon asymmetry on the in-medium behaviour of $Q\bar{Q}$ bound states submerged in the strongly magnetized hot QCD medium. We have reassessed the structure of the gluon two point functions in magnetized thermal medium. We, then evaluate the gluon self-energy and relevant form factors in the frame work of the imaginary-time formalism. Using these form factors, we have calculated the real and imaginary parts of the resummed (full) gluon propagator which will later facilitate the calculation of the (complex) $Q\bar{Q}$ potential. The real-part is plugged into the Schrödinger

equation to get the binding energy whereas the imaginary- part gives the thermal width. At last, we study the effect of quark chemical potential on the quasi-free dissociation of the heavy quarkonia by calculating the dissociation temperatures for the J/ψ and Υ states.

The paper has been organized as follows: In section 2, we have revisited the general covariant tensor structure of the gluon self-energy in the extreme environment of temperature, density and SMF. In subsection 2.1, we calculate the real and imaginary parts of the form factor $b(p_0, p)$ in imaginary- time formalism which give the complex resummed gluon propagator in subsection 3.1. Next, we calculate the medium modification to the complex $Q\bar{Q}$ potential in subsection 3.2. We will discuss the binding energy in subsection 4.1, decay width in 4.2 and will explore the quasi-free dissociation process of J/ψ and Υ in subsection 4.3. Finally, we present the conclusion of this study in section 5.

2 Gluon self-energy tensor and resummed gluon propagator in hot and dense strongly magnetized medium

In this section, we will review the covariant tensor structure of gluon self-energy in magnetized hot and dense QCD medium. The covariant structure is given by [50]

$$\Pi^{\mu\nu}(P) = b(P)B^{\mu\nu}(P) + c(P)R^{\mu\nu}(P) + d(P)M^{\mu\nu}(P) + a(P)N^{\mu\nu}(P), \quad (1)$$

the projection tensors used in the construction of self-energy tensor in Eq. (1) are defined as

$$B^{\mu\nu}(P) = \frac{\bar{u}^\mu \bar{u}^\nu}{\bar{u}^2}, \quad (2)$$

$$R^{\mu\nu}(P) = g_\perp^{\mu\nu} - \frac{P_\perp^\mu P_\perp^\nu}{P_\perp^2}, \quad (3)$$

$$M^{\mu\nu}(P) = \frac{\bar{n}^\mu \bar{n}^\nu}{\bar{n}^2}, \quad (4)$$

$$N^{\mu\nu}(P) = \frac{\bar{u}^\mu \bar{n}^\nu + \bar{u}^\nu \bar{n}^\mu}{\sqrt{\bar{u}^2} \sqrt{\bar{n}^2}}, \quad (5)$$

where $u^\mu = (1, 0, 0, 0)$ is the four velocity of the heat bath and $n_\mu = (0, 0, 0, 1)$ represents the direction of B . \bar{u}^μ and \bar{n}^μ are constructed as

$$\bar{u}^\mu = \left(g^{\mu\nu} - \frac{P^\mu P^\nu}{P^2} \right) u_\nu, \quad (6)$$

$$\bar{n}^\mu = \left(\tilde{g}^{\mu\nu} - \frac{\tilde{P}^\mu \tilde{P}^\nu}{\tilde{P}^2} \right) n_\nu, \quad (7)$$

where $\tilde{g}^{\mu\nu} = g^{\mu\nu} - u^\mu u^\nu$ and $\tilde{P}^\mu = P^\mu - (P \cdot u) u^\mu$. The form factors defined in (1) can be evaluated using the contraction properties as

$$b(P) = B^{\mu\nu}(P) \Pi_{\mu\nu}(P), \quad (8)$$

$$c(P) = R^{\mu\nu}(P) \Pi_{\mu\nu}(P), \quad (9)$$

$$d(P) = M^{\mu\nu}(P) \Pi_{\mu\nu}(P), \quad (10)$$

$$a(P) = \frac{1}{2} N^{\mu\nu}(P) \Pi_{\mu\nu}(P). \quad (11)$$

The general covariant structure of the full gauge boson (gluon) propagator in magnetized hot and dense medium can be written in Landau gauge as [50]

$$D^{\mu\nu}(P) = \frac{(P^2 - d)B^{\mu\nu}}{(P^2 - b)(P^2 - d) - a^2} + \frac{R^{\mu\nu}}{P^2 - c} + \frac{(P^2 - b)M^{\mu\nu}}{(P^2 - b)(P^2 - d) - a^2} + \frac{aN^{\mu\nu}}{(P^2 - b)(P^2 - d) - a^2}. \quad (12)$$

Since, we are interested in the static inter-quark potential, we need only the “00”-component of the full gluon propagator. The “00”-component is given by

$$D^{00}(P) = \frac{(P^2 - d)\bar{u}^2}{(P^2 - b)(P^2 - d) - a^2}, \quad (13)$$

because $R^{00} = M^{00} = N^{00} = 0$. The $Q\bar{Q}$ potential is given by the static limit of the full gluon propagator. Since form factor $a(p_0, p)$ vanishes in the static limit (see the appendix A). The resummed propagator (13) becomes

$$D^{00}(p_0 = 0, p) = -\frac{1}{(p^2 + b(p_0 = 0, p))}. \quad (14)$$

Thus, we are left only with the form factor $b(p_0, p)$ which is needed to be calculated in the static limit. So the next subsection is devoted to the calculation of $b(p_0, p)$.

2.1 Real and imaginary parts of the form factor $b(p_0, p)$

In order to find the complex full gluon propagator, we will work out the real and imaginary parts of the form factor $b(p_0, p)$. Using the contraction property of Eq. (8), $b(p_0, p)$ is given by

$$\begin{aligned}
b(P) &= B^{\mu\nu}(P)\Pi_{\mu\nu}(P), \\
b(P) &= \frac{\bar{u}^\mu \bar{u}^\nu}{\bar{u}^2} \Pi_{\mu\nu}(P), \\
&= \left[\frac{u^\mu u^\nu}{\bar{u}^2} - \frac{(P \cdot u) u^\nu P^\mu}{\bar{u}^2 P^2} - \frac{(P \cdot u) u^\mu P^\nu}{\bar{u}^2 P^2} + \frac{(P \cdot u)^2 P^\nu P^\mu}{\bar{u}^2 P^4} \right] \Pi_{\mu\nu}(P), \\
&= \frac{u^\mu u^\nu}{\bar{u}^2} \Pi_{\mu\nu}(P),
\end{aligned} \tag{15}$$

where we have exploited transversality condition $P^\mu \Pi_{\mu\nu}(P) = P^\nu \Pi_{\mu\nu}(P) = 0$.

We will now evaluate the gluon self-energy in a strong magnetic field at finite temperature and density. As we know only the quark loop gets influenced in SMF while gluon loop will give only thermal contribution. The quark loop contribution to the gluon self-energy is given as

$$\begin{aligned}
\Pi_{\mu\nu}^{ab}(P) &= i \int \frac{d^4 K}{(2\pi)^4} \text{Tr} [gt_b \gamma_\mu S(K) gt_a \gamma_\nu S(Q)], \\
&= \sum_f \frac{ig^2 \delta_{ab}}{2} \int \frac{d^4 K}{(2\pi)^4} \text{Tr} [\gamma_\mu S(K) \gamma_\nu S(Q)],
\end{aligned} \tag{16}$$

where $Q = (K - P)$ and $\text{Tr}(t_a t_b) = \frac{\delta_{ab}}{2}$. The quark propagator $S(K)$ in SMF limit reads as [50, 51]

$$iS(K) = ie^{-\frac{K_\perp^2}{|q_f B|}} \frac{(K_\parallel + m_f)}{(K_\parallel^2 - m_f^2)} (1 - i\gamma_1 \gamma_2), \tag{17}$$

where q_f and m_f refers to the charge and mass of the f^{th} quark flavor, respectively. We choose the metric tensor as

$$\begin{aligned}
g_\parallel^{\mu\nu} &= \text{diag}(1, 0, 0 - 1), \\
g_\perp^{\mu\nu} &= \text{diag}(0, -1, -1, 0),
\end{aligned}$$

and the four-momentum can be decomposed as

$$K_{\parallel}^{\mu} = (k_0, 0, 0, k_z), \quad (18)$$

$$K_{\perp}^{\mu} = (0, k_x, k_y, 0), \quad (19)$$

$$K_{\parallel}^2 = k_0^2 - k_z^2, \quad (20)$$

$$K_{\perp}^2 = k_x^2 + k_y^2, \quad (21)$$

In the SMF, the momentum integration can be decomposed into longitudinal (\parallel) and transverse (\perp) components with respect to the magnetic field, so the gluon self-energy (16) can be factorized into (\parallel) and (\perp) components as

$$\Pi_{\mu\nu}(P) = X(K_{\perp})i \int \frac{d^2 K_{\parallel}}{(2\pi)^2} \text{Tr} \left[\gamma_{\mu} \frac{(K_{\parallel} + m_f)}{(K_{\parallel}^2 - m_f^2)} (1 - i\gamma_1\gamma_2) \gamma_{\nu} \frac{(Q_{\parallel} + m_f)}{(Q_{\parallel}^2 - m_f^2)} (1 - i\gamma_1\gamma_2) \right], \quad (22)$$

where the transverse part is given by

$$\begin{aligned} X(K_{\perp}) &= \sum_f \frac{g^2}{2} \int \frac{d^2 K_{\perp}}{(2\pi)^2} e^{\frac{-K_{\perp}^2 - Q_{\perp}^2}{|q_f B|}}, \\ &= \sum_f e^{-\frac{P_{\perp}^2}{2|q_f B|}} \frac{g^2 |q_f B|}{2\pi}. \end{aligned} \quad (23)$$

In the strong magnetic field ($|q_f B| \gg P_{\perp}^2$), we can approximate $e^{-\frac{P_{\perp}^2}{2|q_f B|}} \approx 1$. After substituting transverse part from Eq. (23), the Eq. (22) becomes,

$$\Pi_{\mu\nu}(P) = - \sum_f \frac{g^2 |q_f B|}{2\pi} T \sum_{k_0} \int \frac{dk_3}{2\pi} \frac{L_{\mu\nu}}{(K_{\parallel}^2 - m_f^2)(Q_{\parallel}^2 - m_f^2)}, \quad (24)$$

where

$$\begin{aligned} L_{\mu\nu} &= u_{\mu}u_{\nu}(k_0q_0 + k_3q_3 + m_f^2) + n_{\mu}n_{\nu}(k_0q_0 + k_3q_3 - m_f^2) \\ &\quad + (u_{\mu}n_{\nu} + n_{\mu}u_{\nu})(k_0q_3 + k_3q_0). \end{aligned} \quad (25)$$

Here the strong coupling g is the function of temperature, chemical potential and magnetic field. It is given by [52]

$$\begin{aligned} \alpha_s(\Lambda^2, eB) &= \frac{g^2}{4\pi} \\ &= \frac{\alpha_s(\Lambda^2)}{1 + b_1 \alpha_s(\Lambda^2) \ln \left(\frac{\Lambda^2}{\Lambda^2 + eB} \right)}, \end{aligned} \quad (26)$$

with

$$\alpha_s(\Lambda^2) = \frac{1}{b_1 \ln \left(\frac{\Lambda^2}{\Lambda_{\overline{MS}}^2} \right)}, \quad (27)$$

where Λ is set at $2\pi\sqrt{T^2 + \frac{\mu^2}{\pi^2}}$ for quarks and $2\pi T$ for gluons, $b_1 = \frac{11N_c - 2N_f}{12\pi}$ and $\Lambda_{\overline{MS}} = 0.176 \text{ GeV}$.

Now substituting $\Pi_{\mu\nu}(P)$ from Eq. (24) in Eq. (15) we get

$$b(P) = - \sum_f \frac{g^2 |q_f B|}{2\pi \bar{u}^2} T \sum_{k_0} \int \frac{dk_3}{2\pi} \frac{(k_0 q_0 + k_3 q_3 + m_f^2)}{(K_{\parallel}^2 - m_f^2)(Q_{\parallel}^2 - m_f^2)}. \quad (28)$$

In the static limit, the real and imaginary parts of $b(p_0, p)$ from the quark loop are obtained as (see the appendix B)

$$\begin{aligned} \text{Re } b(p_0 = 0, p) &= \sum_f \frac{g^2 |q_f B|}{4\pi^2 T} \int_0^\infty dk_3 \left\{ n^+(E_1)(1 - n^+(E_1)) \right. \\ &\quad \left. + n^-(E_1)(1 - n^-(E_1)) \right\} \end{aligned} \quad (29)$$

$$\begin{aligned} \left[\frac{\text{Im } b(p_0, p)}{p_0} \right]_{p_0=0} &= \sum_f g^2 \frac{|q_f B| m_f^2}{16\pi T (\frac{p_3^2}{4} + m_f^2)} \left\{ n^+(\Omega)(1 - n^+(\Omega)) \right. \\ &\quad \left. + n^-(\Omega)(1 - n^-(\Omega)) \right\}, \end{aligned} \quad (30)$$

where $E_1 = \sqrt{k_3^2 + m_f^2}$ and $\Omega = \sqrt{\frac{p_3^2}{4} + m_f^2}$. The distribution functions $n^+(E_1)$ and $n^-(E_1)$ for quarks and anti-quarks, respectively are given as

$$n^\pm(E_1) = \frac{1}{e^{\beta(E_1 \mp \mu)} + 1}. \quad (31)$$

Eq. (30) can be further simplified using the identity

$$n^\pm(E)(1 - n^\pm(E)) = \frac{1}{2(1 + \cosh(\beta(E \mp \mu)))}, \quad (32)$$

as (neglecting $O(\frac{\mu^2}{T^2})$ and higher order terms since we are working in the limit $\mu < T$)

$$\left[\frac{\text{Im } b(p_0, p)}{p_0} \right]_{p_0=0} = \sum_f g^2 \frac{|q_f B| m_f^2}{8\pi T} \frac{1}{p_3^2}. \quad (33)$$

The “00” component of gluon self-energy tensor as a consequence of the gluon-loop is given by [53, 54]

$$\Pi_{00}(p_0, p) = -g^2 T^2 \frac{N_c}{3} \left(\frac{p_0}{2p} \ln \frac{p_0 + p + i\epsilon}{p_0 - p + i\epsilon} - 1 \right), \quad (34)$$

we extract the real and imaginary parts of Eq. (34) which are found to be

$$\text{Re } b_0(p_0 = 0) = g^2 T^2 \left(\frac{N_c}{3} \right), \quad (35)$$

$$\left[\frac{\text{Im } b_0(p_0, p)}{p_0} \right]_{p_0=0} = g^2 T^2 \left(\frac{N_c}{3} \right) \frac{\pi}{2p}. \quad (36)$$

The square of the Debye mass in the strong magnetic field at finite temperature and chemical potential is given by

$$m_D^2 = (b + b_0) \bar{u}^2|_{p_0=0}, \quad (37)$$

$$= m_{\text{q,D}}^2 + m_{\text{g,D}}^2, \quad (38)$$

where the quark-loop contribution ($m_{\text{q,D}}^2$) to the Debye mass is

$$m_{\text{q,D}}^2(T, \mu; B) = \sum_f g^2 \frac{|q_f B|}{4\pi^2 T} \int_0^\infty dk_3 \{n^+(E_1)(1 - n^+(E_1)) + n^-(E_1)(1 - n^-(E_1))\}. \quad (39)$$

It is worthwhile to mention here that the dependence of chemical potential (μ) in $m_{\text{q,D}}$ is only manifested in the finite (physical) quark masses otherwise it simply reduces to the known result [43]

$$m_{\text{q,D}}^2(B) = \sum_f \frac{g^2 |q_f B|}{4\pi^2}. \quad (40)$$

On the other hand, the gluon contribution is as usual given by

$$m_{\text{g,D}}^2(T) = \frac{N_C}{3} g^2 T^2 \quad (41)$$

To visualize the effect of finite baryon asymmetry on the collective modes of a strongly magnetized hot QCD medium, we have plotted the Debye mass (m_D) as a function of

temperature (in units of T_c) with the increasing quark chemical potentials at a fixed magnetic field strength ($eB = 15 m_\pi^2$) (left panel of Fig. 1). We have seen that m_D increases with T , as expected but on the contrary it decreases with μ , which is more significant in the low temperature region [55]. This finding can be better understood if we plot the same with respect to μ at a fixed temperature, $T = 200$ MeV and magnetic field strength, $eB = 15 m_\pi^2$, wherein Debye mass decreases with μ and this trend is pronounced at large μ under consideration. The Debye mass gets reduced in the presence of the strong B in

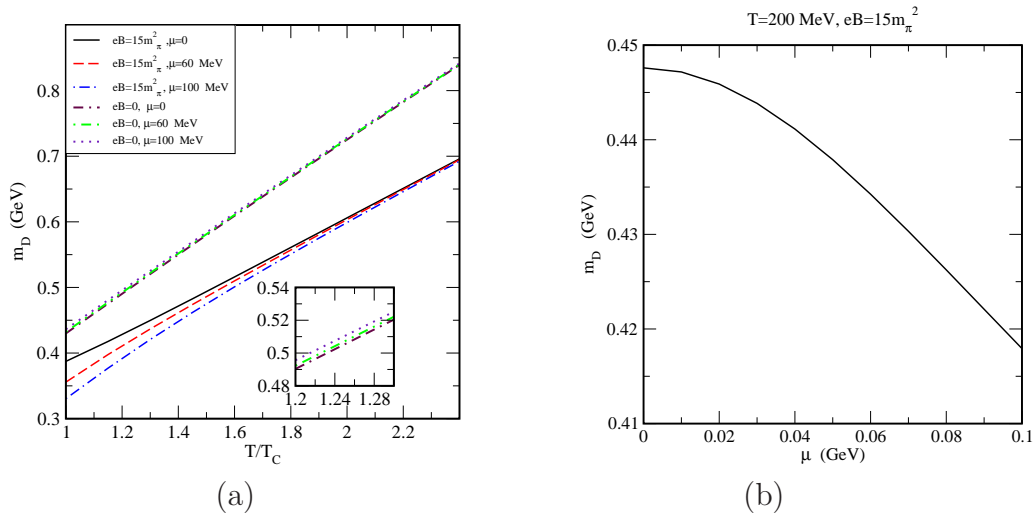


Figure 1: Variation of the Debye mass with the a) temperature, b) quark chemical potential

3 Medium modified $Q\bar{Q}$ potential

In this section, we will explore the effect of surplus of baryons over anti-baryons to the medium modification of $Q\bar{Q}$ potential immersed in a deconfined medium with an ambient strong magnetic field. The inverse Fourier transform of the resummed gluon propagator in

the static limit serves the desired medium-modification in the coordinate space as [56]

$$V(r; T, B, \mu) = C_F g^2 \int \frac{d^3 p}{(2\pi)^3} (e^{ip \cdot r} - 1) D^{00}(p_0 = 0, p), \quad (42)$$

where $C_F (= 4/3)$ is the Casimir factor and $D^{00}(p_0 = 0, p)$ is the static limit of the complex full gluon propagator, whose real and imaginary parts are needed to obtain the complex inter-quark potential. The r -independent term (which is the perturbative free energy of quarkonium at infinite separation) has been subtracted to renormalize the heavy quark free energy.

3.1 The real and imaginary parts of the resummed gluon propagator

The static limit of the real-part of “00”-component of full gluon propagator is given by using Eq. (14) and Eq. (37) as

$$\text{Re } D^{00}(p_0 = 0) = -\frac{1}{p^2 + m_D^2}. \quad (43)$$

Similarly, the imaginary-part reads [57]

$$\text{Im } D^{00}(p_0, p) = \frac{2T}{p_0} \frac{\text{Im } b(p_0, p)}{(P^2 - \text{Re } b(p_0, p))^2 + (\text{Im } b(p_0, p))^2}, \quad (44)$$

which can be further simplified as

$$\text{Im } D^{00}(p_0, p) = 2T \frac{\left[\frac{\text{Im } b(p_0, p)}{p_0} \right]}{(P^2 - \text{Re } b(p_0, p))^2 + \left(p_0 \left[\frac{\text{Im } b(p_0, p)}{p_0} \right] \right)^2}, \quad (45)$$

the above Eq. (45) in static limit ($p_0 = 0$) reduces to

$$\text{Im } D^{00}(p_0 = 0) = 2T \frac{\left[\frac{\text{Im } b(p_0, p)}{p_0} \right]_{p_0=0}}{(p^2 + m_D^2)^2}, \quad (46)$$

where we have exploited $\text{Re } b(p_0 = 0, p) = m_D^2$. Using Eq. (33), the imaginary part of $D^{00}(p_0 = 0, p)$ is given as

$$\text{Im } D^{00}(p_0 = 0, p) = \sum_f \frac{g^2 |q_f B| m_f^2}{4\pi} \frac{1}{p_3^2 (p^2 + m_D^2)^2}. \quad (47)$$

Now, we will revisit the procedure to handle the large distance behaviour of the $Q\bar{Q}$ potential. A phenomenological model has been proposed to study the string part of the potential in [38] where the authors have added a phenomenological nonperturbative term to the HTL full gluon propagator in order to include the effects due to the low frequency modes incorporated in the dimension two gluon condensates. The real and imaginary parts of the phenomenological nonperturbative (NP) term are given by

$$\text{Re } D_{\text{NP}}^{00}(p_0 = 0, p) = -\frac{m_G^2}{(p^2 + m_D^2)^2}, \quad (48)$$

$$\text{Im } D_{\text{NP}}^{00}(p_0 = 0, p) = \frac{2\pi T m_g^2 m_G^2}{p(p^2 + m_D^2)^3}, \quad (49)$$

where the dimension two constant m_G^2 can be expressed in terms of the string tension as $\sigma = \alpha m_G^2/2$. Eqs. (48) and (49) will induce the string contribution in the complex $Q\bar{Q}$ potential. Finally, the real and imaginary parts of the “00”-component of the full gluon propagator can be written as

$$\text{Re } D^{00}(p_0 = 0, p) = -\frac{1}{p^2 + m_D^2} - \frac{m_G^2}{(p^2 + m_D^2)^2}, \quad (50)$$

$$\text{Im } D^{00}(p_0 = 0, p) = \sum_f \frac{g^2 |q_f B| m_f^2}{4\pi} \frac{1}{p_3^2 (p^2 + m_D^2)^2} + \frac{\pi T m_g^2}{p(p^2 + m_D^2)^2} + \frac{2\pi T m_g^2 m_G^2}{p(p^2 + m_D^2)^3} \quad (51)$$

We will use Eqs. (50) and (51) to derive the (complex) $Q\bar{Q}$ potential in the next subsection.

3.2 Real and Imaginary parts of the $Q\bar{Q}$ potential

In this subsection, we will compute the real- and imaginary-parts of inter quark potential between $Q\bar{Q}$ in a strongly magnetized hot quark matter with finite chemical potential by substituting the real- and imaginary-parts of the full gluon propagator, respectively, into the definition (42). Thus, the real-part of $Q\bar{Q}$ potential (with $\hat{r} = r m_D$) is obtained as

$$\text{Re } V(r; T, B, \mu) = -\frac{4}{3} \alpha_s \left(\frac{e^{-\hat{r}}}{r} + m_D(T, \mu, B) \right) + \frac{4}{3} \frac{\sigma}{m_D(T, \mu, B)} (1 - e^{-\hat{r}}), \quad (52)$$

where the dependences of temperature, chemical potential and magnetic field in Debye mass get translated into the medium modified inter-quark potential. The string term in

Eq. (52) comes from the nonperturbative part in Eq. (50). Mainly we wish to visualize the modification due to the sole effect of baryon asymmetry on the real-part of $Q\bar{Q}$ potential as a function of inter-quark distance (r) for increasing μ 's (in Fig. 2). While plotting the real-part, we have abandoned the r -independent terms, which are needed in the potential (52) to obtain its form in $T \rightarrow 0$ limit. In the Fig. 2 (a), we have displayed $\text{Re } V(r; T, B, \mu)$ for $\mu = 0, 60$ and 100 MeV at fixed temperature $T = 200$ MeV and strong magnetic field $eB = 15 m_\pi^2$. We have observed that the real-part becomes more attractive at finite chemical potential in comparison to $\mu = 0$. This strong nature of the $Q\bar{Q}$ potential can be attributed to the less screening in the presence of baryon asymmetry ($\mu \neq 0$) in the strongly magnetized QCD medium. We have displayed the $\text{Re } V(r; T, B, \mu)$ considering the same values of μ at $T = 250$ MeV (in the Fig. 2 (b)) and have found the same behavior. It is evident from the Fig 2 (b) that as the temperature rises the effect of μ diminishes.

We will now evaluate the imaginary-part of the inter-quark potential using the imaginary-part of full gluon propagator from Eq. (51) into Eq. (42), which is separable into perturbative and nonperturbative (NP) parts as

$$\text{Im } V(r; T, B, \mu) = \text{Im } V_{\text{perturbative}}(r; T, B, \mu) + \text{Im } V_{\text{NP}}(r; T, B, \mu). \quad (53)$$

The perturbative part is separated into quark-loop (q) and gluon-loop (g) contributions as

$$\text{Im } V_{\text{perturbative}}(r; T, B, \mu) = \text{Im } V_q(r; T, B, \mu) + \text{Im } V_g(r; T, B, \mu), \quad (54)$$

where the quark-loop contribution has been calculated as

$$\begin{aligned} \text{Im } V_q(r, T, B, \mu) = & \sum_f \alpha_s g^2 m_f \frac{|q_f B|}{3\pi^2} \left[\frac{\pi}{2m_D^3} - \frac{\pi e^{-\hat{r}}}{2m_D^3} - \frac{\pi \hat{r} e^{-\hat{r}}}{2m_D^3} \right. \\ & \left. - \frac{2\hat{r}}{m_D} \int_0^\infty \frac{p dp}{(p^2 + m_D^2)^2} \int_0^{pr} \frac{\sin t}{t} dt \right]. \end{aligned} \quad (55)$$

and the gluon-loop contribution is

$$\text{Im } V_g(r; T, B, \mu) = -\frac{4}{3} \frac{\alpha_s T m_g^2}{m_D^2} \psi_1(\hat{r}), \quad (56)$$

where the function $\psi_1(\hat{r})$ is given by [38, 46]

$$\psi_1(\hat{r}) = 2 \int_0^\infty \frac{z dz}{(z^2 + 1)^2} \left[1 - \frac{\sin z \hat{r}}{z \hat{r}} \right], \quad (57)$$

which can be further simplified in the small \hat{r} limit as

$$\psi_1(\hat{r}) \approx -\frac{1}{9} \hat{r}^2 (3 \ln \hat{r} - 4 + 3\gamma_E). \quad (58)$$

Similarly, we calculate the imaginary-part of the string part of the $Q\bar{Q}$ potential using the nonperturbative term in the full gluon propagator from Eq. (51) in Eq. (42), we get

$$\text{Im } V_{\text{NP}}(r; T, B, \mu) = -\frac{16\sigma T m_g^2}{3m_D^4} \psi_2(\hat{r}), \quad (59)$$

where the function $\psi_2(\hat{r})$ is given in [38, 46]

$$\psi_2(\hat{r}) = 2 \int_0^\infty \frac{z dz}{(z^2 + 1)^3} \left[1 - \frac{\sin z \hat{r}}{z \hat{r}} \right], \quad (60)$$

which further takes the form in limit ($\hat{r} \ll 1$)

$$\psi_2(\hat{r}) \approx \frac{\hat{r}^2}{12} + \frac{\hat{r}^4}{900} (15 \ln \hat{r} - 23 + 15\gamma_E). \quad (61)$$

While the real-part will explore the effect of baryon asymmetry on the binding energy, the effect on the dissociation will be understood through the imaginary-part (in Fig. 3). The magnitude of imaginary-part is found to decrease in baryon asymmetric matter, $\mu \neq 0$, compared to its counterpart at $\mu = 0$ and it decreases further as μ rises. We have conducted a similar investigation at $T = 250$ MeV in the Fig. 3 (b) and have found the same behavior, however the effect of quark chemical potential on imaginary-part is less pronounced at high temperatures because the effect of the μ on the Debye mass is not much visible.

Now we will compare our results of the $Q\bar{Q}$ potential in the presence of the strong magnetic field ($eB = 15m_\pi^2$) with those in the absence of magnetic field ($B = 0$). The real and imaginary parts of the resummed gluon propagator (in the static limit) are given in the absence of magnetic field as

$$\text{Re } D^{00}(p_0 = 0, p) = -\frac{1}{p^2 + m_D'^2} - \frac{m_G^2}{(p^2 + m_D'^2)^2}, \quad (62)$$

$$\text{Im } D^{00}(p_0 = 0, p) = \frac{\pi T m_D'^2}{p(p^2 + m_D'^2)^2} + \frac{2\pi T m_D'^2 m_G^2}{p(p^2 + m_D'^2)^3}. \quad (63)$$

respectively. Using Eq. (42), the real and imaginary parts of $Q\bar{Q}$ potential are found to be

$$\text{Re } V(r; T, \mu) = -\frac{4}{3}\alpha'_s \left(\frac{e^{-\hat{r}}}{r} + m'_D \right) + \frac{4}{3} \frac{\sigma}{m'_D} (1 - e^{-\hat{r}}), \quad (64)$$

$$\text{Im } V(r; T, \mu) = -\frac{4}{3}\alpha'_s T \psi_1(\hat{r}) - \frac{16\sigma T}{3m_D'^2} \psi_2(\hat{r}), \quad (65)$$

respectively. Here α' is the strong coupling constant, which is given by

$$\alpha'_s(T) = \frac{6\pi}{(33 - 2N_f) \ln \left(\frac{Q}{\Lambda_{QCD}} \right)}, \quad (66)$$

where $Q = 2\pi\sqrt{T^2 + \frac{\mu^2}{\pi^2}}$ and m'_D is the Debye mass, which reads as

$$m_D'^2 = g'^2 T^2 \left\{ \frac{N_c}{3} + \frac{N_f}{6} \left(1 + \frac{3\mu^2}{\pi^2 T^2} \right) \right\}. \quad (67)$$

We notice from Fig 1 (a) that magnitude of the Debye mass in the absence of B is greater in comparison to that in strong B environment. So the real part of the potential gets screened at higher amount and becomes less attractive in comparison to $B \neq 0$ case. [seen in Fig. 2 (a)]. Similar observation we notice when the temperature of the medium is 250 MeV [seen in Fig. 2 (b)]. On the other hand, the magnitude of the imaginary part gets enhanced in comparison to $B \neq 0$ case [seen in Fig. 3 (a) and (b)]. The impact of μ on the Debye mass (and hence on the $Q\bar{Q}$ potential) in the absence of magnetic field is not much visible for $\mu = 60$ and 100 MeV. The Debye mass gets slightly increased as the strength of μ is raised. Consequently, the real part becomes less attractive and the magnitude of the imaginary part increases.

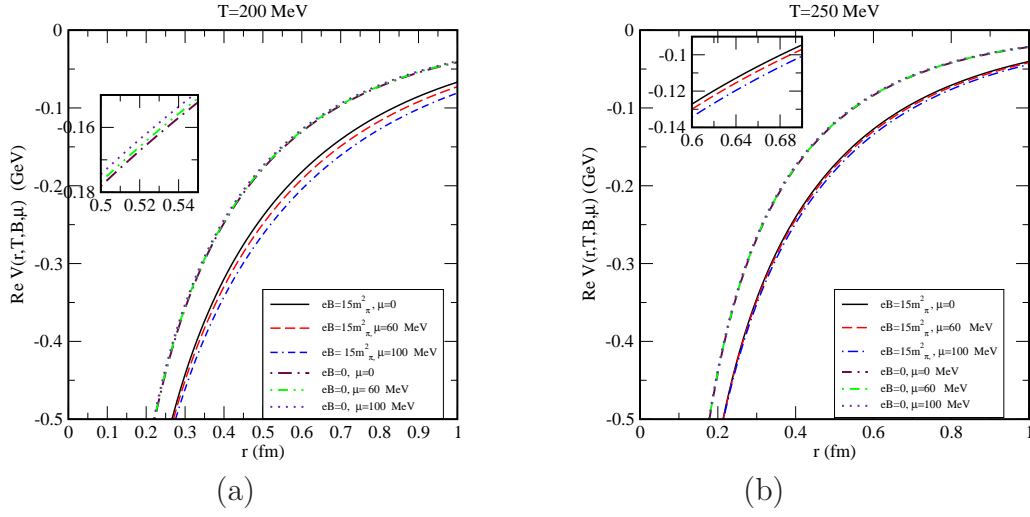


Figure 2: Variation of $\text{Re } V(r, T, B, \mu)$ with inter-quark separation (r) at different strengths of the quark chemical potential (μ).

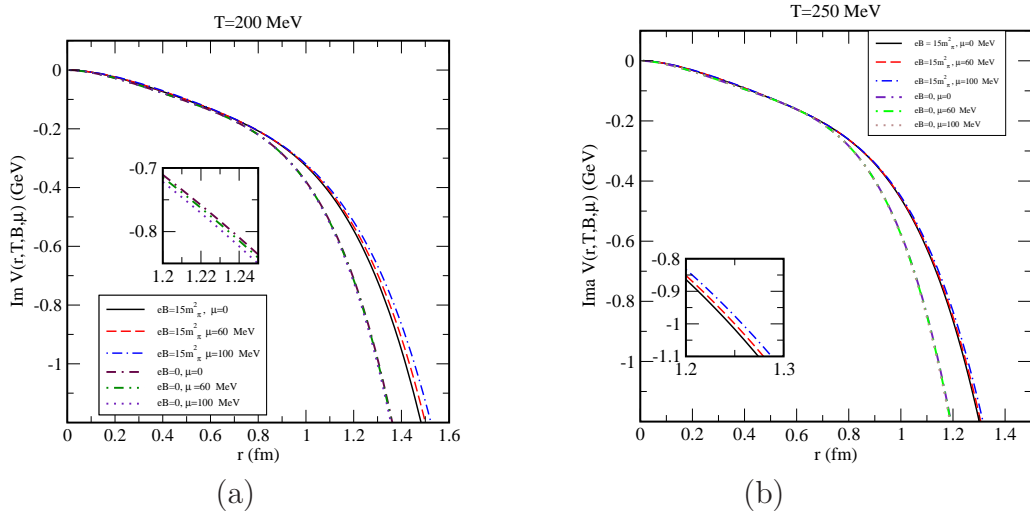


Figure 3: Variation of $\text{Im } V(r, T, B, \mu)$ with inter-quark separation (r) at different strengths of the quark chemical potential (μ).

4 Properties of quarkonia

We will now explore how the presence of the baryon asymmetry in the strongly magnetized hot QCD medium affects the properties of heavy quarkonia. We will compute the binding energy and decay width of the $Q\bar{Q}$ system with the help of the real and imaginary parts of the $Q\bar{Q}$ potential, respectively.

4.1 Binding energy (BE)

We have solved the radial part of the Schrödinger equation numerically exploiting the real-part of the potential to obtain the energy eigenvalues which are utilized to calculate the binding energy of quarkonia. We have examined the effect of quark chemical potential on the binding energy of the heavy quarkonium states in Fig. 4. For that purpose, we have computed the BE of J/ψ and Υ at $\mu = 0, 60$ and 100 MeV while fixing $eB = 15m_\pi^2$. We have observed that BE decreases with T , which is justified since the screening mass increases with T . The magnitude of the binding energy is slightly higher for $\mu \neq 0$ in comparison to $\mu = 0$ case. This behavior can be understood in terms of the softening of the screening mass in the presence of the baryon asymmetry in the medium which leads to the stronger nature of the real-part of inter-quark potential hence slightly enhanced values of the binding energy.

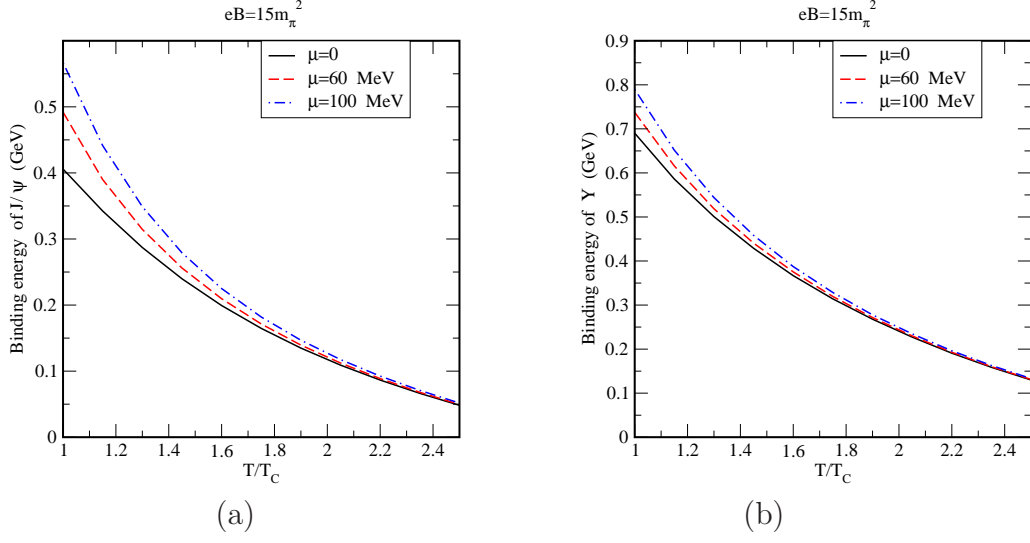


Figure 4: Variation of binding energy of J/ψ (a) and Υ (b) with T at different strengths of the quark chemical potential (μ).

4.2 Thermal width

We will now explore the broadening of the thermal width of the $Q\bar{Q}$ bound states in a strongly magnetized hot QCD medium through the imaginary part of the $Q\bar{Q}$ potential. In small distance limit, the imaginary part of the potential can be treated as the perturbation to the vacuum potential which gives the thermal width (Γ) for a particular resonance state as

$$\Gamma(T, B, \mu) = -2 \int_0^\infty \text{Im } V(r; T, B, \mu) |\Psi(r)|^2 d\tau, \quad (68)$$

where we choose $\Psi(r)$ as the Coloumbic wave function which reads

$$\Psi(r) = \frac{1}{\sqrt{\pi a_0^3}} e^{-r/a_0}. \quad (69)$$

Here a_0 refers to the Bohr radius of the $Q\bar{Q}$ bound state.

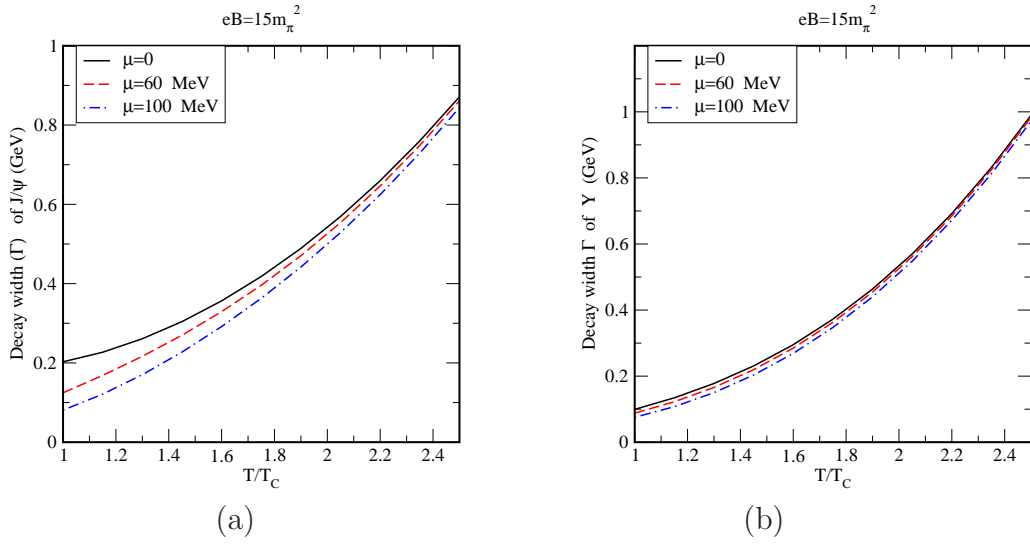


Figure 5: Variation of Decay width of J/ψ (a) and Υ (b) with T (in units of T_c) at different strengths of μ .

In order to decipher the effect of the finite chemical potential on the thermal width (Γ) of the $Q\bar{Q}$ bound states, we have evaluated Γ numerically for J/ψ and Υ with respect to T (in Fig. 5) for $\mu = 0, 60$ and 100 MeV. We have observed that Γ increases with the temperature while it gets decreased in the presence of baryon asymmetry ($\mu \neq 0$) in the medium. This behavior can be explained in terms of $\text{Im } V(r; T, B, \mu)$ whose magnitude gets decreased in the presence of μ .

4.3 Dissociation of quarkonia

In this section we will study the dissociation process of the $Q\bar{Q}$ bound states in a baryon asymmetric strongly magnetized thermal QCD medium and will see how the dissociation temperature (T_D) of quarkonia is affected by the presence of finite amount of μ . We have used the criterion (Γ): $\Gamma \geq 2$ binding energy [58] to evaluate the values of the dissociation points for J/ψ and Υ .

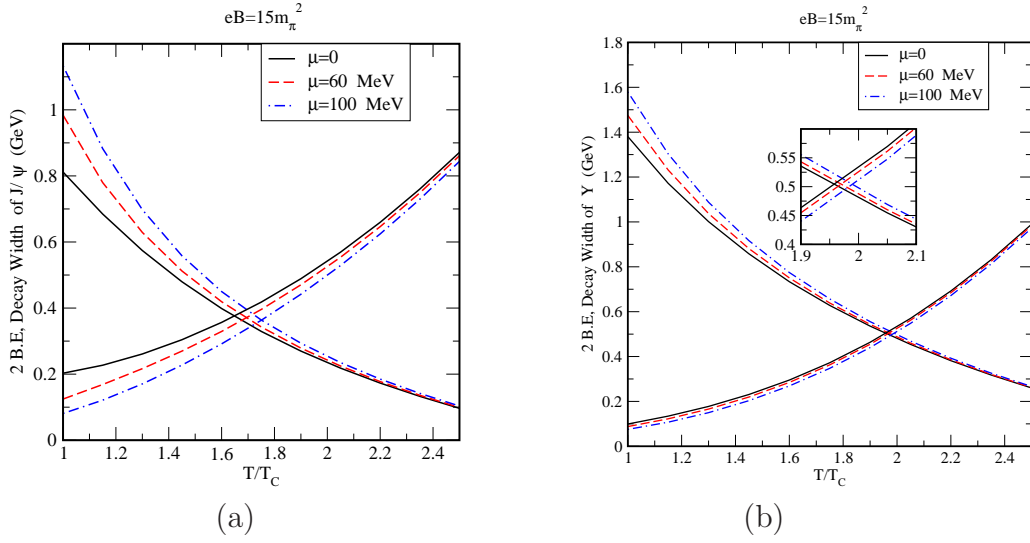


Figure 6: Competition between the Γ and $2 \times$ BE for J/ψ (a) and Υ (b) with respect to T at different strengths of the quark chemical potential (μ)

	T_D (in terms of T_c), $eB = 15 m_\pi^2$	
State	J/ψ	Υ
$\mu = 0$	1.64	1.95
$\mu = 60$	1.69	1.97
$\mu = 100$	1.75	2.00

Table 1: T_D 's of J/ψ and Υ at different strengths of chemical potential (μ).

We have plotted thermal width and twice of the binding energy with the temperature in Fig. 6 and have found that T_D 's of J/ψ and Υ increase slightly in baryon asymmetric QCD medium in comparison to baryonless ($\mu = 0$) medium. The dissociation temperatures for J/ψ are found to be $1.64 T_c$, $1.69 T_c$, and $1.75 T_c$ at the $\mu = 0, 60$ and 100 MeV respectively whereas Υ is dissociated at $1.95 T_c$, $1.97 T_c$ and $2.00 T_c$ for $\mu = 0, 60$ and 100 MeV respectively.

5 Conclusions

To conclude, we have examined the effects of quark chemical potential on the properties of the quarkonia in baryon asymmetric strongly magnetized hot QCD medium. First, we have given a revisit to the general covariant tensor structure of gluon self-energy in above mentioned medium and computed the relevant form factors. We use these form factors in the calculation of the (complex) full gluon propagator which further get translated into the (complex) $Q\bar{Q}$ potential. We have added a phenomenological non-perturbative term induced by the dimension two gluon condensate to the usual HTL resummed propagator to evaluate the medium modification to string part of the $Q\bar{Q}$ potential. The real-part becomes more attractive while magnitude of the imaginary-part gets decreased in the baryon asymmetric medium. We evaluate the binding energy of the $Q\bar{Q}$ bound states solving the Schrödinger equation numerically considering the real-part of the potential whereas the imaginary-part gives the thermal width. The binding energy of J/ψ and Υ get enhanced while decay width gets decreased at finite μ in comparison to baryonless medium ($\mu = 0$). This increment in the binding energy is attributed to the stronger nature of the $Q\bar{Q}$ potential in presence of μ . we have finally explored the dissociation process of heavy quark bound states in the above mentioned medium and observed that T_D 's for J/ψ and Υ now attains slightly higher values in the baryon asymmetric medium. J/ψ is dissociated at $1.64 T_c$, $1.69 T_c$ and $1.75 T_c$ for $\mu = 0, 60, 100$ MeV, respectively whereas Υ is dissociated at $1.95 T_c$, $1.97 T_c$ and $2.00 T_c$ for the same strengths of μ . This study leads to the conclusion that baryon asymmetry in strongly magnetized hot QCD medium prevents slightly early dissociation of quarkonia in comparison to baryonless medium.

Acknowledgements

One of us BKP acknowledges the financial assistance from the CSIR (Grant No.03 (1407)/17/EMR-II), Government of India.

Appendices

We present explicit calculation of the form factor $a(p_0, p)$ and $b(p_0, p)$ in the following appendices.

A Calculation of the form factor $a(P)$

We will calculate the form factor $a(p_0, p)$ using the imaginary time formalism of the finite temperature field theory. We can write from Eq. (11)

$$\begin{aligned}
a(p_0, p) &= i \sum_f \frac{g^2 |q_f B|}{2\pi} \frac{p_0 p_3}{\sqrt{\bar{u}^2} \sqrt{\bar{n}^2} \tilde{P}^2} \int \frac{d^2 K_{\parallel}}{(2\pi)^2} \frac{[k_0^2 + k_3^2 + m_f^2]}{(K_{\parallel}^2 - m_f^2)(Q_{\parallel}^2 - m_f^2)} \\
&= - \sum_f \frac{g^2 |q_f B|}{2\pi} \frac{p_0 p_3}{\sqrt{\bar{u}^2} \sqrt{\bar{n}^2} \tilde{P}^2} T \sum_{k_0} \int \frac{dk_3}{2\pi} \frac{[k_0^2 + k_3^2 + m_f^2]}{(K_{\parallel}^2 - m_f^2)(Q_{\parallel}^2 - m_f^2)} \\
&= - \sum_f \frac{g^2 |q_f B|}{2\pi} \frac{p_0 p_3}{\sqrt{\bar{u}^2} \sqrt{\bar{n}^2} \tilde{P}^2} T \sum_{k_0} \int \frac{dk_3}{2\pi} \left(\frac{1}{(K_{\parallel}^2 - m_f^2)} + \frac{2(k_3^2 + m_f^2)}{(K_{\parallel}^2 - m_f^2)(Q_{\parallel}^2 - m_f^2)} \right) \\
&= - \sum_f \frac{g^2 |q_f B|}{2\pi} \frac{p_0 p_3}{\sqrt{\bar{u}^2} \sqrt{\bar{n}^2} \tilde{P}^2} (I_1(P) + I_2(P))
\end{aligned} \tag{A.70}$$

where

$$\begin{aligned}
I_1(P) &= T \sum_{k_0} \int \frac{dk_3}{2\pi} \frac{1}{(K_{\parallel}^2 - m_f^2)}, \\
&= - \int \frac{dk_3}{2\pi} \frac{(1 - n^+(E_1) - n^-(E_1))}{2E_1},
\end{aligned} \tag{A.71}$$

the first term gives the nonleading contribution in T , retaining only leading order term we get

$$I_1(P) = \int \frac{dk_3}{2\pi} \frac{(n^+(E_1) + n^-(E_1))}{2E_1}, \tag{A.72}$$

where $n^+(E_1)$ and $n^-(E_1)$ are the distribution function for the quarks and anti quarks, respectively and are given as

$$n^+(E_1) = \frac{1}{e^{\beta(E_1-\mu)} + 1} \quad (\text{A.73})$$

$$n^-(E_1) = \frac{1}{e^{\beta(E_1+\mu)} + 1}. \quad (\text{A.74})$$

Now taking the second term in (A.70)

$$\begin{aligned} I_2(P) &= T \sum_{k_0} \int \frac{dk_3}{2\pi} \frac{2(k_3^2 + m_f^2)}{(K_{\parallel}^2 - m_f^2)(Q_{\parallel}^2 - m_f^2)}, \\ &= - \int \frac{dk_3}{2\pi} \frac{2(k_3^2 + m_f^2)}{4E_1 E_2} \left(\frac{(1 - n^+(E_1) - n^-(E_2))}{(i\omega - E_1 - E_2)} + \frac{(n^-(E_1) - n^-(E_2))}{(i\omega + E_1 - E_2)} \right. \\ &\quad \left. + \frac{(n^+(E_1) - n^+(E_2))}{(i\omega - E_1 + E_2)} - \frac{(1 - n^-(E_1) - n^+(E_2))}{(i\omega + E_1 + E_2)} \right), \end{aligned} \quad (\text{A.75})$$

where $E_1 = \sqrt{k_3^2 + m_f^2}$ and $E_2 = \sqrt{(k_3 - p_3)^2 + m_f^2}$. In the HTL approximation the Eq. (A.75) reduces to

$$I_2(P) = - \int \frac{dk_3}{2\pi} \left(\frac{n^+(E_1) + n^-(E_1)}{2E_1} - \frac{dn^-(E_1)}{dE_1} \frac{p_3}{2(p_0 + p_3)} + \frac{dn^+(E_1)}{dE_1} \frac{p_3}{2(p_0 - p_3)} \right) \quad (\text{A.76})$$

Adding (A.72) and (A.76)

$$I_1(P) + I_2(P) = - \int \frac{dk_3}{2\pi} \left(\frac{dn^+(E_1)}{dE_1} \frac{p_3}{2(p_0 - p_3)} - \frac{dn^-(E_1)}{dE_1} \frac{p_3}{2(p_0 + p_3)} \right). \quad (\text{A.77})$$

Now putting $(I_1(P) + I_2(P))$ in (A.70) we get the form factor $a(P)$ as

$$\begin{aligned} a(p_0, p) &= \sum_f \frac{g^2 |q_f B|}{2\pi} \frac{p_0 p_3}{\sqrt{\tilde{n}^2} \sqrt{\tilde{u}^2} \tilde{P}^2} \int \frac{dk_3}{2\pi} \left(\frac{dn^+(E_1)}{dE_1} \frac{p_3}{2(p_0 - p_3)} - \frac{dn^-(E_1)}{dE_1} \frac{p_3}{2(p_0 + p_3)} \right) \\ &= - \sum_f \frac{g^2 |q_f B|}{2\pi T} \frac{p_0 p_3}{\sqrt{\tilde{n}^2} \sqrt{\tilde{u}^2} \tilde{P}^2} \int \frac{dk_3}{2\pi} \left(n^+(E_1)(1 - n^+(E_1)) \frac{p_3}{2(p_0 - p_3)} \right. \\ &\quad \left. - n^-(E_1)(1 - n^-(E_1)) \frac{p_3}{2(p_0 + p_3)} \right), \end{aligned} \quad (\text{A.78})$$

which vanishes in the static limit ($p_0 = 0$).

B Calculation of the form factor $b(p_0, p)$

We can write from Eq. (28) using HTL approximation

$$\begin{aligned}
b(p_0, p) &= - \sum_f \frac{g^2 |q_f B|}{2\pi \bar{u}^2} T \sum_{k_0} \int \frac{dk_3}{2\pi} \frac{[k_0^2 + k_3^2 + m_f^2]}{(K_{\parallel}^2 - m_f^2)(Q_{\parallel}^2 - m_f^2)}, \\
&= - \sum_f \frac{g^2 |q_f B|}{2\pi \bar{u}^2} T \sum_{k_0} \int \frac{dk_3}{2\pi} \left(\frac{1}{(K_{\parallel}^2 - m_f^2)} + \frac{2(k_3^2 + m_f^2)}{(K_{\parallel}^2 - m_f^2)(Q_{\parallel}^2 - m_f^2)} \right), \\
&= - \sum_f \frac{g^2 |q_f B|}{2\pi \bar{u}^2} (I_1(P) + I_2(P)), \tag{B.79}
\end{aligned}$$

putting the value of $(I_1(P) + I_2(P))$ from eq. (A.77) in (B.79), the form factor $b(P)$ can be written as

$$b(p_0, p) = \sum_f \frac{g^2 |q_f B|}{2\pi \bar{u}^2} \int \frac{dk_3}{2\pi} \left(\frac{dn^+(E_1)}{dE_1} \frac{p_3}{2(p_0 - p_3)} - \frac{dn^-(E_1)}{dE_1} \frac{p_3}{2(p_0 + p_3)} \right). \tag{B.80}$$

The real part of the form factor $b(P)$ is given by

$$\begin{aligned}
\text{Re } b(p_0, p) &= - \sum_f \frac{g^2 |q_f B|}{4\pi^2 \bar{u}^2 T} \int dk_3 \left\{ n^+(E_1)(1 - n^+(E_1)) \frac{p_3}{2(p_0 - p_3)} \right. \\
&\quad \left. - n^-(E_1)(1 - n^-(E_1)) \frac{p_3}{2(p_0 + p_3)} \right\}. \tag{B.81}
\end{aligned}$$

We have calculated the imaginary part of the form factor $b(p_0, p)$ using the identity

$$\text{Im } b(p_0, p) = \frac{1}{2i} \lim_{\eta \rightarrow 0} [b(p_0 + i\epsilon, p) - b(p_0 - i\epsilon, p)], \tag{B.82}$$

along with the formula which gives the discontinuity across the real axis as

$$\frac{1}{2i} \left(\frac{1}{p_0 + \sum_j E_j + i\epsilon} - \frac{1}{p_0 + \sum_j E_j - i\epsilon} \right) = -\pi \delta(p_0 + \sum_j E_j). \tag{B.83}$$

Thus using the above identities Eq. (B.82) and Eq. (B.83), the imaginary-part of $b(p_0, p)$ is found to be

$$\text{Im } b(p_0, p) = g^2 \frac{|q_f B| m_f^2 p_0}{16\pi T (\frac{p_3^2}{4} + m_f^2)} \left\{ n^+(\Omega)(1 - n^+(\Omega)) + n^-(\Omega)(1 - n^-(\Omega)) \right\}, \tag{B.84}$$

where $\Omega = \sqrt{\frac{p_3^2}{4} + m_f^2}$.

References

- [1] I. Arsene et al., BRAHMS Collaboration, Nucl. Phys. A **757**,1 (2005).
- [2] K. Adcox et al., PHENIX Collaboration, Nucl. Phys. A **757**, 184 (2005).
- [3] F. Carminati et al., ALICE Collaboration, J. Phys. G: Nucl. Part. Phys. **30**, 1517 (2004).
- [4] B. Alessandro et al., ALICE Collaboration, J. Phys. G: Nucl. Part. Phys. **32**, 1295 (2006).
- [5] P. Senger, Cent. Eur. J. Phys. **10**, 1289 (2012)
- [6] V. Skokov, A. Illarionov, V. Toneev, Int. J. Mod. Phys. A **24**, 5925 (2009).
- [7] V. Voronyuk, V. D. Toneev, W. Cassing, E. L. Bratkovskaya, V. P. Konchakovski, S.A. Voloshin, Phys. Rev. C **83**, 054911 (2011).
- [8] K. Tuchin, Adv. High Energy Phys. **2013**, 490495 (2013).
- [9] L. McLerran, V. Skokov, Nucl. Phys. A **929**, 184 (2014).
- [10] S. Rath and B. K. Patra, Phys. Rev. D **100**, 016009 (2019).
- [11] A. Bandyopadhyay, B. Karmakar, N. Haque, M.G. Mustafa, Phys. Rev. D **100**, 034031 (2019).
- [12] S. Rath, B. K. Patra, JHEP **1712**, 098 (2017).
- [13] S. Rath, B. K. Patra, Eur. Phys. J. A **55**, 220 (2019).
- [14] B. Karmakar, R. Ghosh, A. Bandyopadhyay, N. Haque, M.G.Mustafa, Phys. Rev. D **99**, 094002 (2019)
- [15] Kenji Fukushima, Dmitri E. Kharzeev and Harmen J. Warringa, Phys. Rev. D **78**, 074033 (2008).

- [16] V. Braguta, M. N. Chernodub, V. A. Goy, K. Landsteiner, A. V. Molochkov and M. I. Polikarpov, Phys. Rev. D **89**, 074510 (2014).
- [17] Dmitri E. Kharzeev and Dam T. Son, Phys. Rev. Lett. **106**, 062301 (2011).
- [18] V. P. Gusynin, V. A. Miransky and I. A. Shovkovy, Phys. Rev. Lett. **73**, 3499 (1994).
- [19] P. Braun-Munzinger, J. Stachel, J. Phys. G **28**, 1971 (2002)10.
- [20] J. Cleymans, J. Phys. G **35**, 044017 (2008)11.
- [21] A. Andronic et al., Nucl. Phys. A **837**, 65 (2010).
- [22] K. Fukushima, Y. Hidaka, Phys. Rev. Lett. **117**, 102301 (2016).
- [23] M. Hasan, B. K. Patra, B. Chatterjee, P. Bagchi, Nucl. Phys. A **995**, 121688 (2020).
- [24] G.T. Bodwin, E. Braaten, G.P. Lepage, Phys. Rev. D **51**, 1125 (1995).
- [25] N. Brambilla, A. Pineda, J. Soto, and A. Vairo, Nucl. Phys. B **566**, 275 (2000).
- [26] W. M. Alberico, A. Beraudo, A. De Pace and A. Molinari, Phys. Rev. D **77**, 017502 (2008).
- [27] M. Laine, O. Philipsen, and M. Tassler, P. Romatschke, J. High Energy Phys. **03**, 054 (2007).
- [28] T. Matsui, H. Satz, Phys. Lett. B **178**, 416 (1986).
- [29] A. Beraudo, J. P. Blaizot, C. Ratti, Nucl. Phys. A **806**, 312 (2008).
- [30] N. Brambilla, M. A. Escobedo, J. Ghiglieri, A. Vairo, JHEP **1305**, 130 (2013).
- [31] L. Thakur, U. Kakade, B. K. Patra, Phys. Rev. D **89**, 094020 (2014).
- [32] L. Thakur, N. Haque, U. Kakade, B. K. Patra, Phys. Rev. D **88**, 054022 (2013).
- [33] A. Dumitru, Y. Guo, M. Strickland, Phys. Rev. D **79**, 114003 (2009).

- [34] B. K. Patra, H. Khanchandani, L. Thakur, Phys. Rev. D **92**, 085034 (2015).
- [35] B. K. Patra, H. Khanchandani, Phys. Rev. D **91**, 066008 (2015).
- [36] A. Rothkopf, T. Hatsuda, S. Sasaki, Phys. Rev. Lett. **108**, 162001 (2012).
- [37] D. Lafferty and A. Rothkopf Phys. Rev. D **101**, 056010 (2020).
- [38] Y. Guo, L. Dong, J. Pan, and M. R. Moldes, Phys. Rev. D **100**, 036011 (2019).
- [39] J. Alford and M. Strickland, Phys. Rev. D **88**, 105017 (2013).
- [40] C. Bonati, M. D’Elia, and A. Rucci, Phys. Rev. D **92**, 054014 (2015).
- [41] C. Bonati, M. D’Elia, M. Mariti, M. Mesiti, F. Negro, A. Rucci, and F. Sanfilippo, Phys. Rev. D **94**, 094007 (2016).
- [42] C. Bonati, M. D’Elia, M. Mariti, M. Mesiti, F. Negro, A. Rucci, and F. Sanfilippo, Phys. Rev. D **95**, 074515 (2017).
- [43] M. Hasan, B. Chatterjee, B. K. Patra, Eur. Phys. J. C **77**, 767 (2017).
- [44] B. Singh, L. Thakur, H. Mishra, Phys. Rev. D **97**, 096011 (2018).
- [45] S. A. Khan, B. K. Patra and M. Hasan, arXiv:2004.08868[hep-ph].
- [46] M. Hasan, B. K. Patra Phys. Rev. D **102**, 036020 (2020).
- [47] M. Hasan, B. K. Patra Int. J. Mod. Phys. A **36** (2021) 06, 2150045.
- [48] B. Singh, S. Mazumder and H. Mishra, JHEP **2005**, 068 (2020). .
- [49] B. Singh, M. Kurian, S. Mazumder, H. Mishra, V. Chandra and S. K. Das, arXiv:2004.11092[hep-ph].
- [50] B. Karmakar, A. Bandyopadhyay, N. Haque and M. G. Mustafa, Eur. Phys. J. C. **79**, 658, (2019).

- [51] T. Chyi et al., Phys. Rev. D **62**, 105014 (2000).
- [52] A. Ayala, C. A. Dominguez, S. Hernandez-Ortiz, L. A. Hernandez, M. Loewe, D. Manreza Paret, and R. Zamora, Phys. Rev. D **98**, 031501 (2018).
- [53] H. A. Weldon, Phys. Rev. D **26**, 1394 (1982).
- [54] R. D. Pisarski, Phys. Rev. Lett. **63**, 1129 (1989).
- [55] Uttam Kakade and Binoy Krishna Patra, Phys. Rev. C **92**, 024901 (2015).
- [56] Adrian Dumitru, Yun Guo, and Michael Strickland Phys. Rev. D **79**, 114003 (2009).
- [57] H. A. Weldon, Phys. Rev. D **42**, 2384 (1990).
- [58] A. Mocsy and P. Petreczky, Phys. Rev. Lett. **99**, 211602 (2007).